Electronic Supplementary Material (ESI) for Physical Chemistry Chemical Physics.

Supporting Information

Realizing Semiconductor – Half-Metal Transition in Zigzag Graphene Nanoribbons Supported on Hybrid Fluorographene-Graphane Nanoribbons

Shaobin Tang[1,*] and Xinrui Cao[2]

[1]*Key Laboratory of Organo-Pharmaceutical Chemistry of Jiangxi Province, Gannan Normal University, Ganzhou 341000, China*
[2]*Department of Theoretical Chemistry and Biology, School of Biotechnology, Royal Institute of Technology, S-106 91 Stockholm, Sweden*

[*] *E-mail address:* tsb1980@xmu.edu.cn

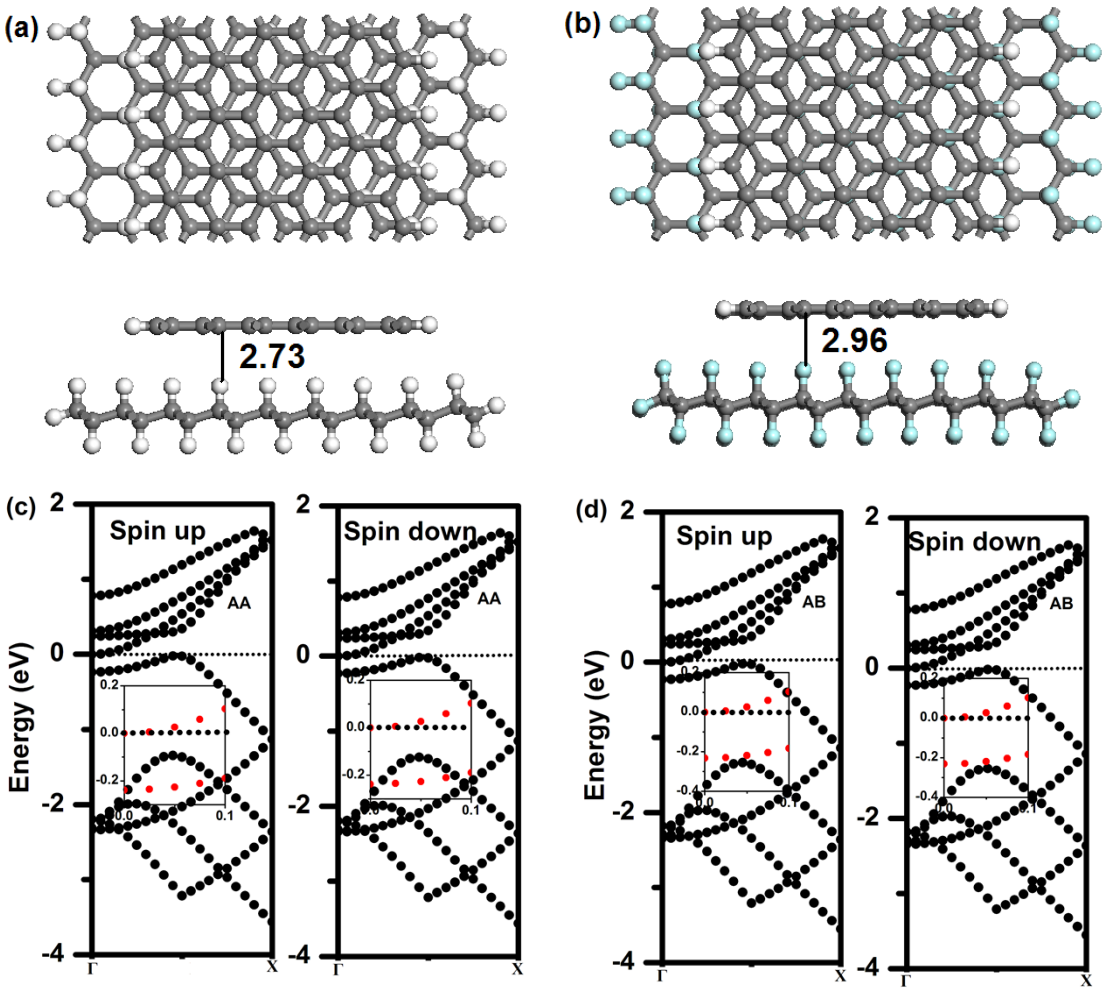

Figure S1. Top and side views of geometric structures of (a) 6-ZGNR/9H-G and (b) 6-ZGNR/9F-G in AB stacking pattern. Spin-polarized band structures of 6-ZGNR/9F-G in (c) AA and (d) AB stacking. The Fermi level is set to zero. The insert in (c) and (d) shows the bands near the Fermi level.

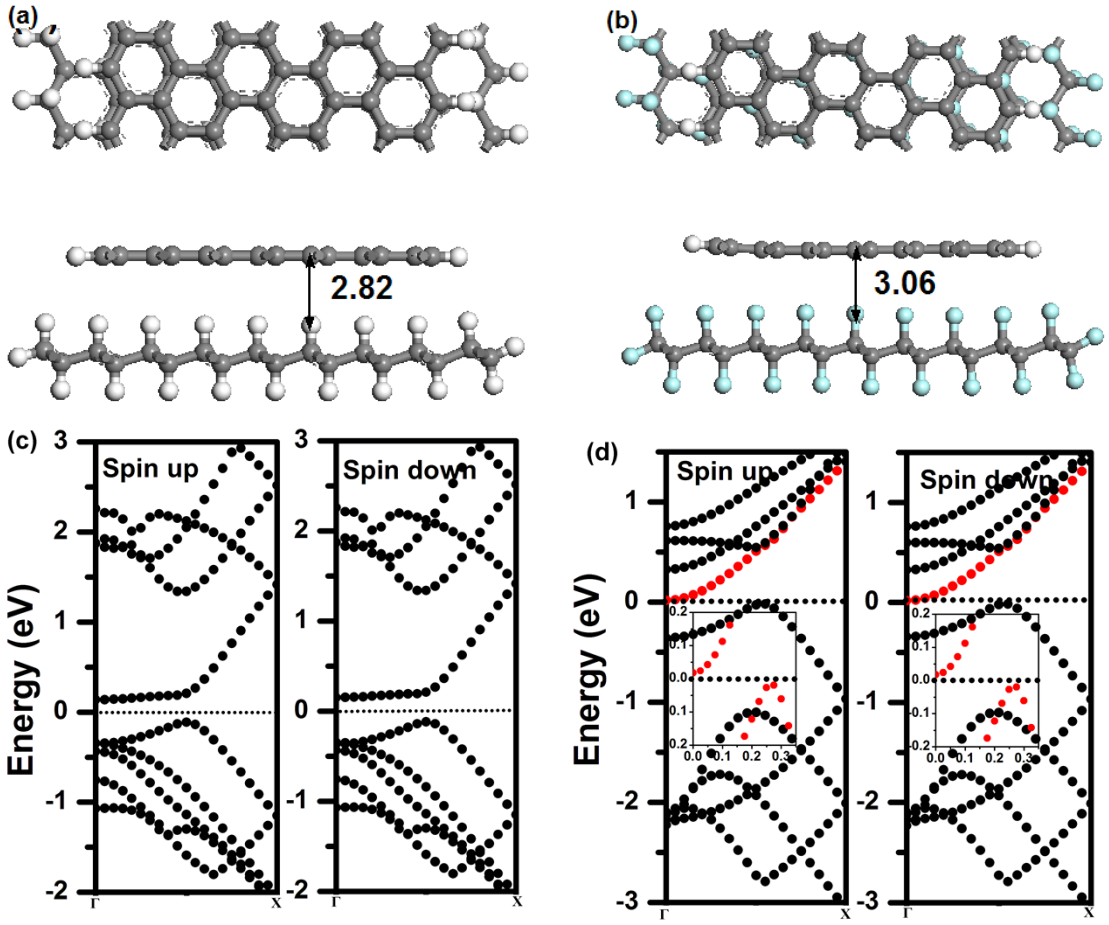

Figure S2. Top and side views of geometric structures (a, b) and spin-polarized band structures (c, d) by PBE with vdW correction. (a) and (c) 9-ZGNR/9H-G, and (b) and (d) 9-ZGNR/9F-G. The interlayer distances in (a) and (b) are in Å. The Fermi level is set to zero, and the insert in (d) shows the bands near the Fermi level.

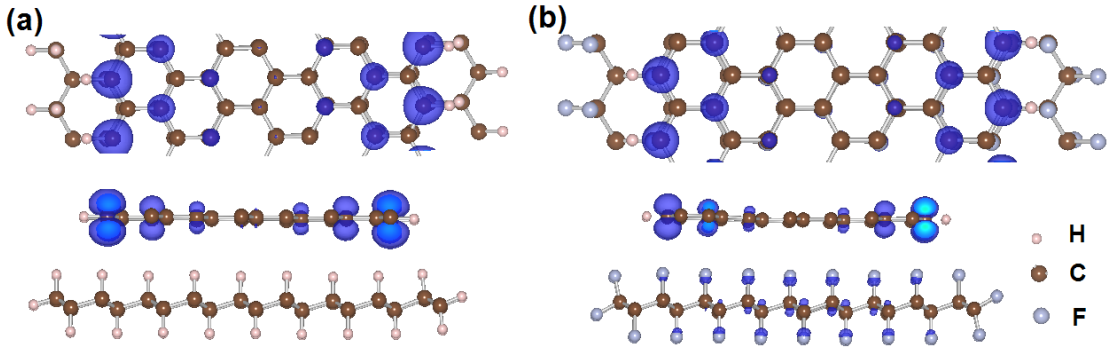

Figure S3. The partial charge densities of (a) 7-ZGNR/9H-G and (b) 7-ZGNR/9F-G in AFM state within energy range $|E - E_f| \leq 0.2$ eV. The isosurface is 0.002 e/Å^3.

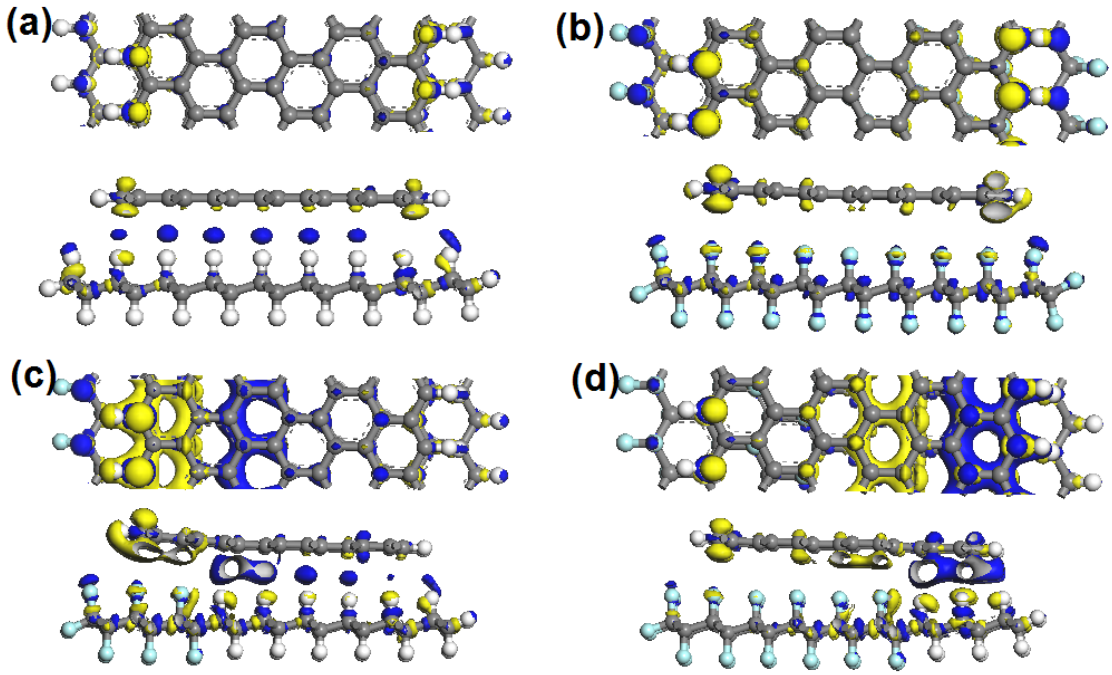

Figure S4. Charge density difference of (a) 7-ZGNR/9H-G, (b) 7-ZGNR/9F-G, (c) 7-ZGNR/6H-3F-G, and (d) 7-ZGNR/3H-6F-G. The blue and yellow areas denote electron accumulation and depletion, respectively, and isosurfaces are 0.002 e/Å^3.

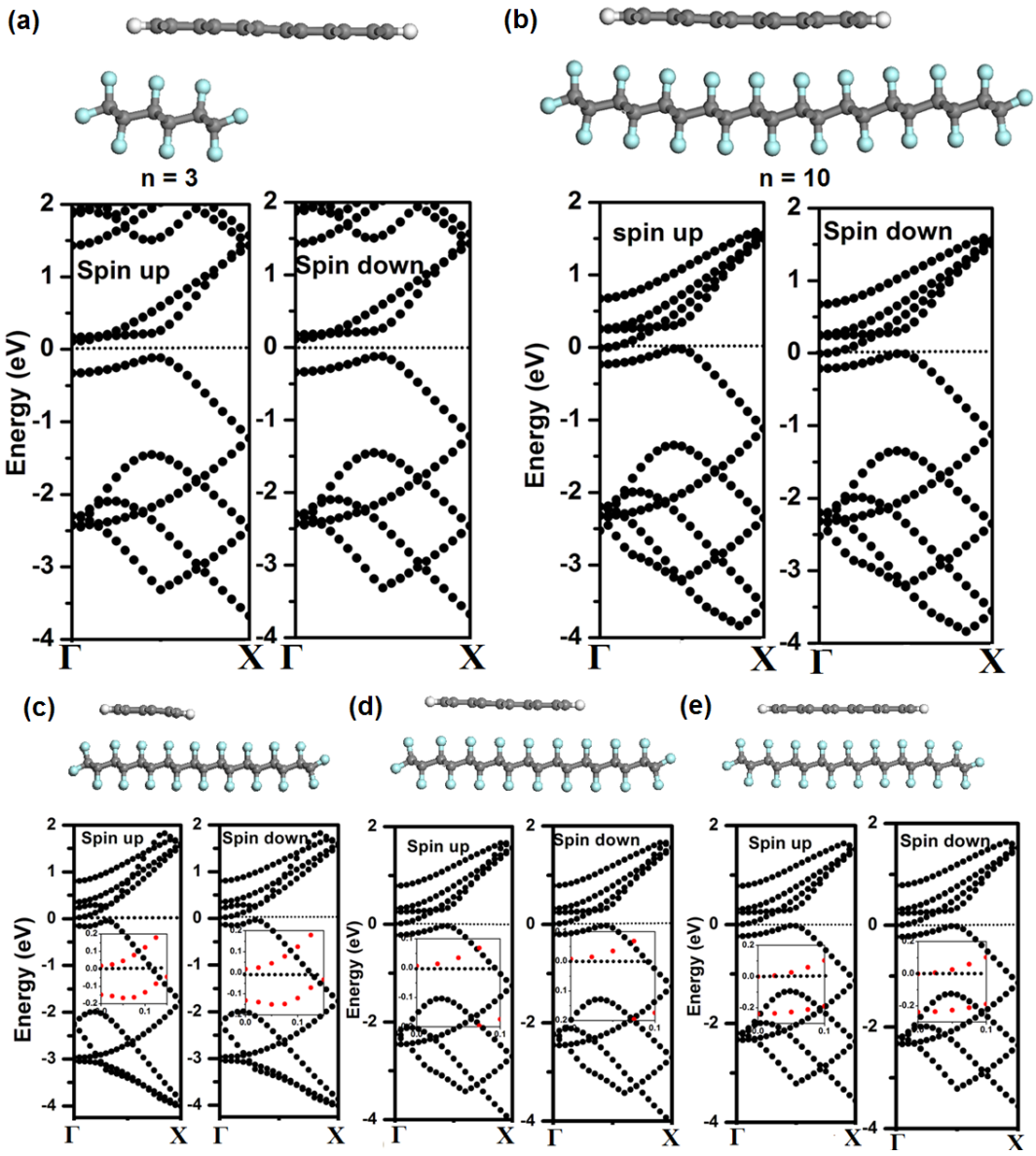

Figure S5. Side view of geometric structures (top panel) and band structures (bottom panel) of (a) 6-ZGNR/3F-G, (b) 6-ZGNR/10F-G, (c) 3-ZGNR/9F-G, (d) 5-ZGNR/9F-G, and (e) 6-ZGNR/9F-G. The Fermi level is set to 0.

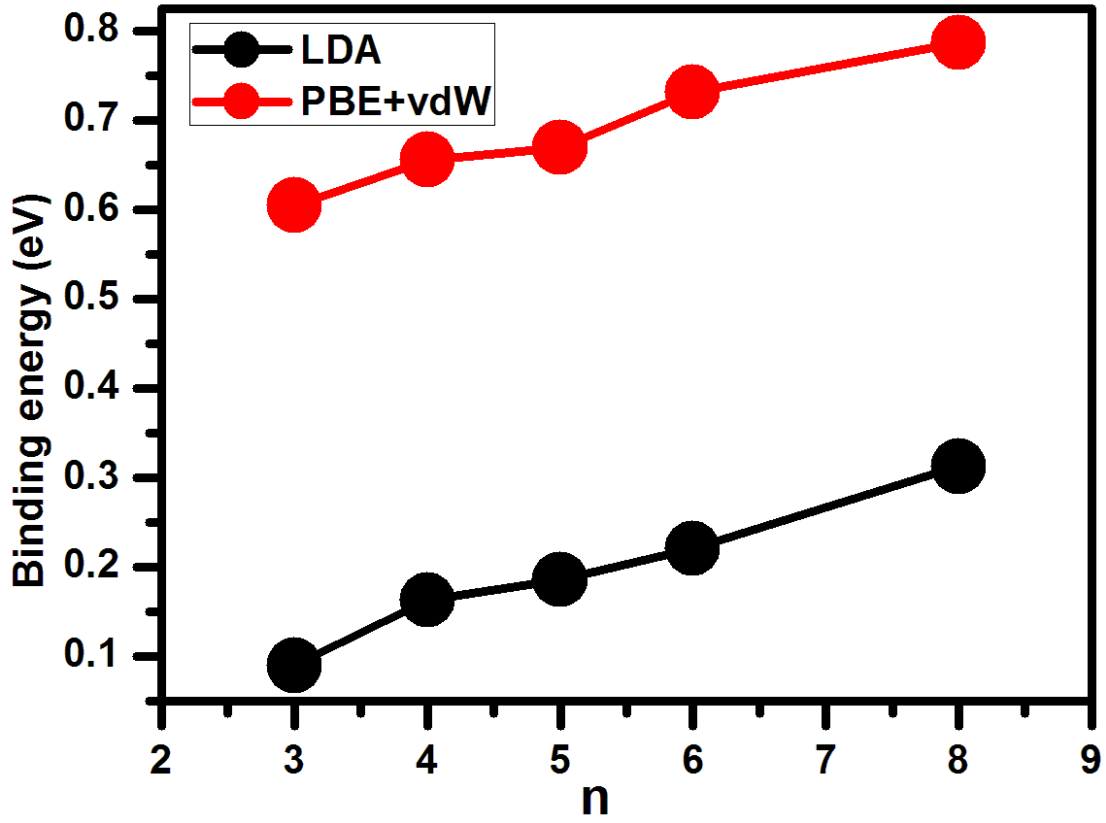

Figure S6. The binding energy of 6-ZGNR/nF-G as a function of the number of fluorinated zigzag chains n in support by both LDA and PBE+vdW.

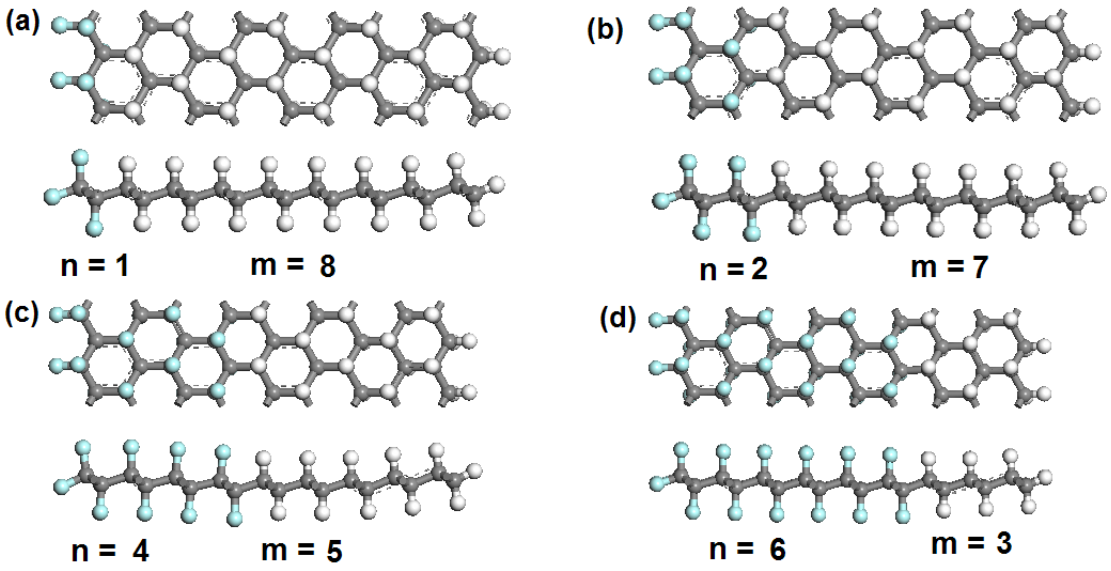

Figure S7. Top and side views of geometric structures of (9-**n**)H-**n**F-G with n = (a) 1, (b) 2, (c) 4, and (d) 6.

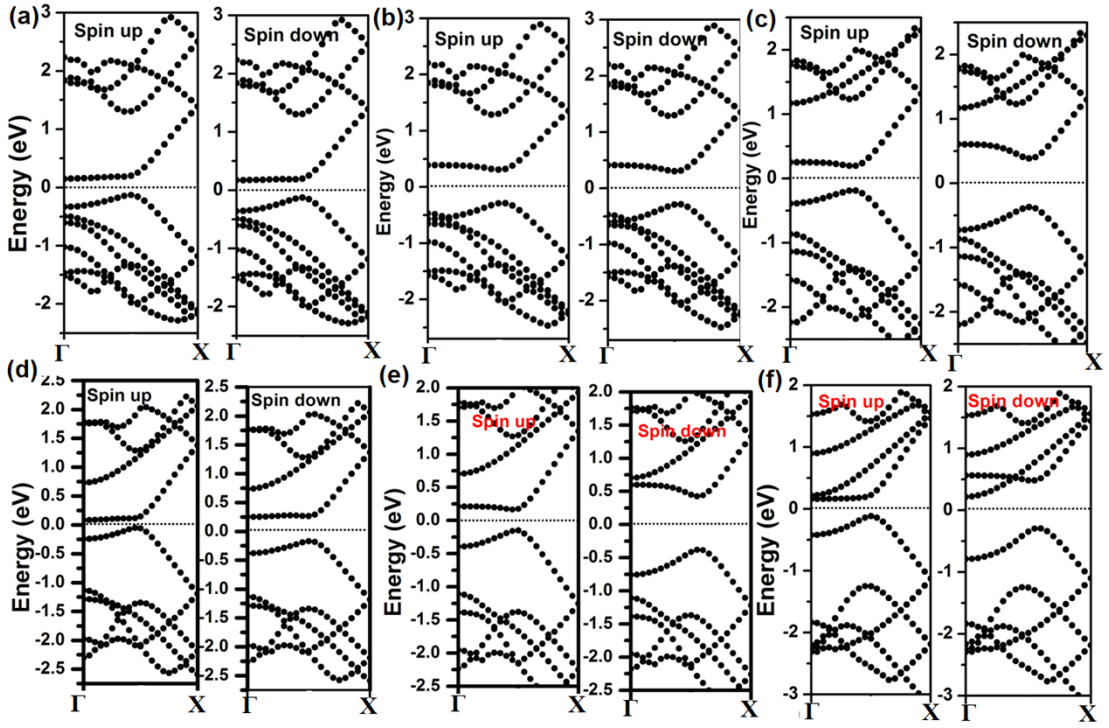

Figure S8. Spin-polarized band structures of 7-ZGNR/(9-**n**)H-**n**F-G by (a, d) LSDA and (b, c, e, and f) PBE+D. (a) and (b) **n** = 1, (c) **n** = 3, (d) and (e) **n** = 4, and (f) **n** = 6. The Fermi level is set to zero.

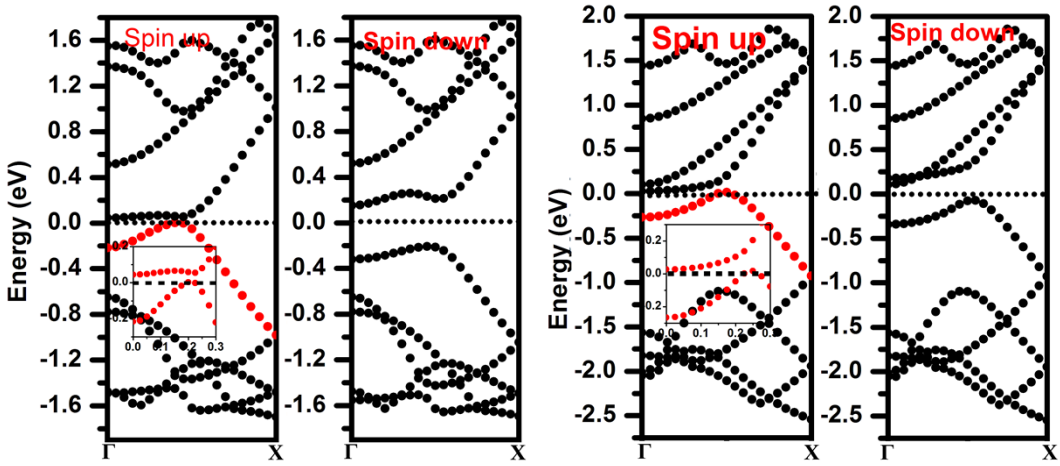

Figure S9. Spin-polarized band structures of 7-ZGNR/6H-3F-G and 7-ZGNR/3H-6F-G with interlayer spacing of 1.65 and 2.21 Å, respectively. The Fermi level is set to 0.

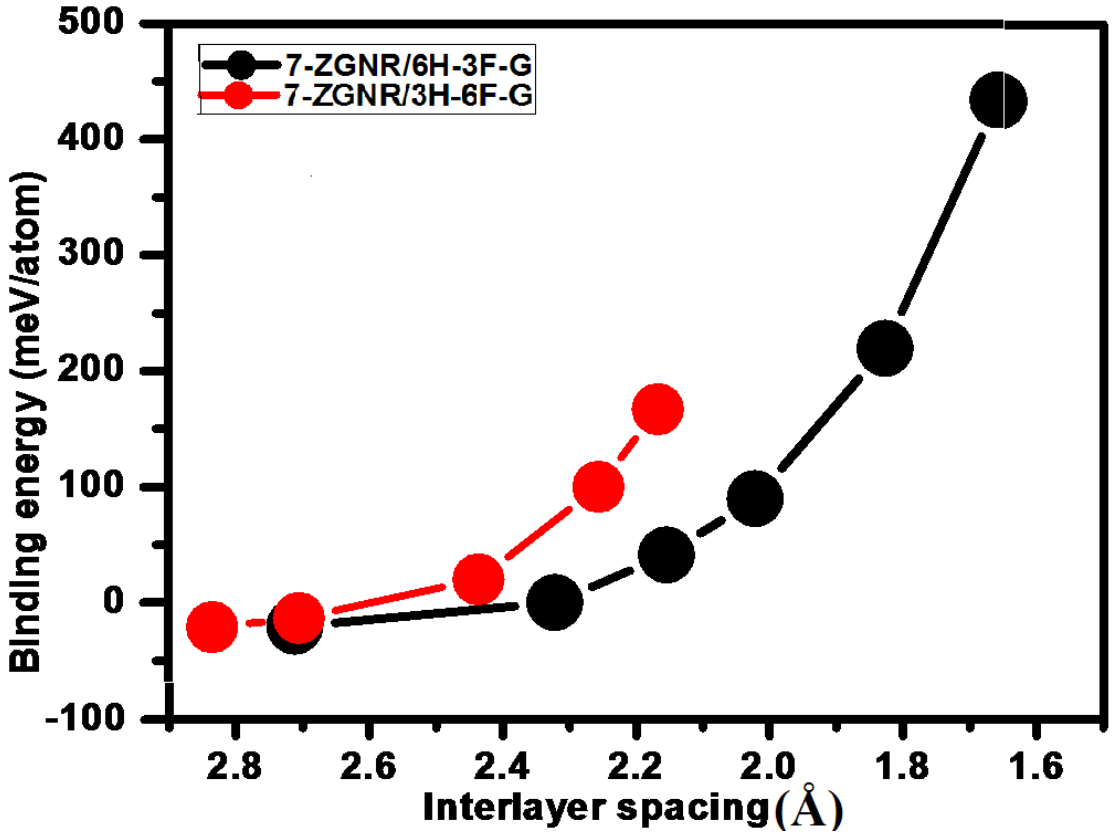

Figure S10. The binding energy of 7-ZGNR/6H-3F-G and 3H-6F-G as a function of the interlayer spacing.